J|A|C|S ARTICLES

Published on Web 05/10/2010

An Electrochemical Scanning Tunneling Microscopy Study of 2-(6-Mercaptoalkyl)hydroquinone Molecules on Au(111)

Paolo Petrangolini,[†,‡] Andrea Alessandrini,[†,‡] Lorenzo Berti,[†,#] and Paolo Facci*[,†]

Centro S3, CNR-Istituto di Nanoscienze, Via Campi 213/A, 41125 Modena, Italy, and Department of Physics, University of Modena and Reggio Emilia, Via Campi 213/A, 41125 Modena, Italy

Received February 26, 2010; E-mail: paolo.facci@unimore.it

Abstract: The hydroquinone/benzoquinone redox couple involves the exchange of two electrons and two protons in its oxidation/reduction reaction in aqueous buffered solutions. In this work, we employed Electrochemical Scanning Tunneling Microscopy and Spectroscopy (EC-STM, EC-STS) to study the interfacial electron transfer properties of hydroquinone incorporated in a Self Assembled Monolayer on a Au(111) substrate. The exchange of electrons between the STM tip and the substrate is regulated by the redox levels of the sandwiched molecule and showed the presence of two regions of tunneling enhancement in the tunneling current/overvoltage relationship. The two regions can be attributed to the presence of two one-electron transfer processes whose equilibrium positions shift upon pH variations. This is the first time a redox molecule involving the exchange of both electrons and protons is studied by EC-STM and EC-STS. The hydroquinone/benzoquinone redox couple can be exploited to obtain an electrochemically or a pH gated transistor.

1. Introduction

Achieving control over the conductivity of a single molecule positioned between two nanometer-spaced electrodes represents currently a major experimental focus in molecular electronics.[1,2] Many approaches have been developed to probe molecular conductivity at the single molecule level. Among these, scanning probe microscopies (SPMs) offer the captivating possibility of coupling imaging and spectroscopic measurements. In the large family of SPMs, the most suitable techniques for such purpose are Scanning Tunneling Microscopy (STM)[3−6] and Conductive-Atomic Force Microscopy (C-AFM).[7,8] STM, in its Electrochemical Scanning Tunneling Microscopy (EC-STM)[9,10] configuration, enables the investigation of tunneling currents (I_t) in liquid environment, allowing the study of molecules whose oxidation state can be modulated electrochemically. In this arrangement, molecules are positioned between a conductive substrate and the STM tip and two possible strategies have been developed to establish electrical contact between the components. In the *symmetric configuration*, both electrodes (substrate and the tip) are covalently bound to the molecule.[11] In the *asymmetric configuration*, the molecule is covalently bound only to the substrate while the tip is separated from the molecule by a tunneling junction. EC-STM has been exploited to study the conductive behavior of porphyrins,[10] transition metal complexes,[12−14] ferrocenyl-derivatives,[15] carotenes,[16] molecular wires containing viologen-moieties,[17,18] and the redox metalloproteins azurin[19−23] and cytochrome c.[24] Many of these studies revealed the dependence of I_t on the substrate potential at

[†] Centro S3, CNR-Istituto di Nanoscienze.
[‡] University of Modena and Reggio Emilia.
[#] Present address: Department of Internal Medicine, Division of Hematology and Oncology, University of California, Davis Health System, Sacramento, CA 95817.

(1) Aviram, A.; Ratner, M. A. *Chem. Phys. Lett.* **1974**, *29*, 277–283.
(2) Nitzan, A.; Ratner, M. A. *Science* **2003**, *300*, 1384–1389.
(3) Binnig, G.; Rohrer, H.; Gerber, C.; Weibel, E. *Phys. Rev. Lett.* **1982**, *49*, 57–61.
(4) *Scanning Tunneling Microscopy and Spectroscopy: Theory, Techniques, and Applications*; Bonnell, D. A., Ed.; VCH Verlagsgesellschaft: Weinheim, 1993.
(5) Chen, C. J. *Introduction to Scanning Tunneling Microscopy*; Oxford University Press: New York, 1993.
(6) Haiss, W.; van Zalinge, H.; Higgins, S. J.; Bethell, D.; Hobenreich, H.; Schiffrin, D. J.; Nichols, R. J. *J. Am. Chem. Soc.* **2003**, *125*, 15294–15295.
(7) Cui, X. D.; Primak, A.; Zarate, X.; Tomfohr, J.; Sankey, O. F.; Moore, A. L.; Moore, T. A.; Gust, D.; Harris, G.; Lindsay, S. M. *Science* **2001**, *294*, 571–574.
(8) Zhao, J. W.; Davis, J. J.; Sansom, M. S. P.; Hung, A. *J. Am. Chem. Soc.* **2004**, *126*, 5601–5609.
(9) Siegenthaler, H.; Christoph, R. In *Scanning Tunneling Microscopy and Related Methods*; Behm, R. J., Garcia, N., Rohrer, H., Eds.; Kluwer Academic Publishers: Dordrecht, Boston, 1990; Vol. 184, pp 315−333.
(10) Tao, N. J. *Phys. Rev. Lett.* **1996**, *76*, 4066–4069.
(11) Xu, B.; Tao, N. J. *Science* **2003**, *301*, 1221–1223.
(12) Albrect, T.; Guckian, A.; Ulstrup, J.; Vos, J. G. *Nano Lett.* **2005**, *5*, 1451–1455.
(13) Albrecht, T.; Moth-Poulsen, K.; Christensen, J. B.; Guckian, A.; Bjørnholm, T.; Vos, J. G.; Ulstrup, J. *Faraday Discuss.* **2006**, *131*, 265–279.
(14) Albrecht, T.; Guckian, A.; Ulstrup, J.; Vos, J. G. *IEEE Trans. Nanotechnol.* **2005**, *4*, 430–434.
(15) Yokota, Y.; Fukui, K.; Enoki, T. *J.Phys. Chem. C* **2007**, *111*, 7561–7564.
(16) Visoly-Fisher, I.; Daie, K.; Terazono, Y.; Herrero, C.; Fungo, F.; Otero, L.; Durantine, E.; Silber, J. J.; Sereno, L.; Gust, D.; Moore, T.; Moore, A. L.; Lindsay, S. M. *Proc. Natl. Acad. Sci. U.S.A.* **2006**, *103*, 8686–8690.
(17) Li, Z.; Han, B.; Meszaros, G.; Pobelov, I.; Wandlowski, T.; Blaszczyk, A.; Mayor, M. *Faraday Discuss.* **2006**, *131*, 121–143.
(18) Pobelov, I. V.; Li, Z.; Wandlowski, T. *J. Am. Chem. Soc.* **2008**, *130*, 16045–16054.
(19) Facci, P.; Alliata, D.; Cannistraro, S. *Ultramicroscopy* **2001**, *89*, 291–298.

constant bias. The observed behavior mirrored a resonance with a maximum near the redox midpoint of the molecule. Those experiments also opened the possibility of implementing an electrochemically gated transistor, where the electrochemical potential of the solution can be used as the gate.[21] This gating is made possible through the alignment of the redox states of the molecule with the Fermi levels of the electrodes, resulting in tunneling enhancement.

Along with EC-STM studies on redox-active molecules, several groups have also elaborated theories to elucidate the conduction mechanism observed in the EC-STM experimental setup.[25−27] It has been noted that the electronic levels of electrochemically active molecules are strongly coupled to the environment, and as a result, the energies of oxidized and reduced states at equilibrium are separated by twice the reorganization energy of the molecule, λ. This value represents the free energy associated with the electron transfer reaction. When electrons tunnel from the tip to the substrate (or vice versa) through the molecular redox states, the tunneling efficiency is dependent on the alignment of all the electronic levels involved and on the rate of each interfacial electron transfer. The latter is defined by the nature of the coupling between the molecule and the electrodes. Multiple scenarios have been proposed to describe the entire electron transfer process based on the mechanism of each interfacial electron transfer step (between the tip and the molecule and between the molecule and the substrate). These include the following: resonant tunneling considering[27] or disregarding[28] the stochastic population of the redox levels; noncoherent two-step electron transfer with complete relaxation of the molecule between the two steps;[29] or a two-step electron transfer with a partial vibrational relaxation.[30] Which of these models best fits the experimental data can be established based on the dependence of I_t on the potential of one electrode while keeping the bias constant or, alternatively, on the dependence of I_t on the applied bias while keeping the potential of one electrode fixed. Unfortunately, neither approach is completely accurate because many factors implicated in the electron transfer mechanism are not easy to discern. For example, the effective potential at the molecule redox site in the tunneling gap can be strongly affected by the applied bias between tip and substrate (i.e., the two working electrodes). As a consequence, the equilibrium redox potential measured through voltammetric studies can be different from the effective equilibrium redox potential.[22] The different mechanisms imply a different position of the maximum in the tunneling current as function of the potential of the working electrode on which the molecule is adsorbed. Moreover, in some scenarios, two maxima are expected,[30] based on the possibility that the molecule is initially oxidized or reduced, corresponding to electrons or holes transport. Because of these difficulties, in many experimental studies, where an enhancement of the tunneling current is observed, the mechanism underlying the observed behavior is still under debate.

Theoretical approaches have mainly focused on single electron transfer mediated by a molecule bearing a single redox level. Very recently, theoretical studies for a two-electron transfer process for a molecule with only one redox level have been reported.[31,32] The main result of these simulations was the prediction of two peaks in the I_t versus gate voltage relation. This behavior can be justified by two different perspectives underlying the same physical mechanism: the presence of a Coulomb blockade effect allowing the transfer of the second electron only when a specific electrode potential is reached, or the presence of two different chemical species characterized by a one-electron transfer occurring at different electrode potentials.

Two strategies can be applied to study I_t in the metal/redox molecule/metal configuration in an EC-STM setup. In the pioneering work by Tao,[10] the spectroscopy-like imaging approach was used. There, a series of images of the same sample area at the same applied bias but for different values of the substrate potential were acquired at constant tunneling current. An enhancement of the tunneling current was reflected in a variation of the apparent height of the imaged molecules. This method allowed the direct visualization of the molecules involved in the redox-mediated tunneling mechanism, but a direct measurement of the tunneling current was not permitted. Following another strategy, termed Electrochemical Scanning Tunneling Spectroscopy (EC-STS), the tip is brought into close proximity to the sample until a specified current set point is reached. At that point, the *z*-feedback is switched off and the potential of the working electrode on which the molecule is adsorbed is swept. In this approach, the correlation of the tunneling current on the potential is directly obtained and the results are easier to compare even to theoretical models.[21,33]

In this work, we relied on both EC-STM and EC-STS to study the behavior of hydroquinone molecules covalently bound to a Au(111) electrode. The hydroquinone moieties have been incorporated in a Self Assembled Monolayer (SAM) on gold through an alkylic linker terminating with a thiol group. The electrochemical properties of the hydroquinone/benzoquinone redox couple have been extensively studied in the context of its biological role in electron transport processes.[34] The redox chemistry of the hydroquinone/quinone couple can be described as a $2e^-$ plus $2H^+$ reaction in protic environment, as the quinone-to-hydroquinone reaction consumes protons. The overall reaction from quinone to hydroquinone can be illustrated by a nine-membered square scheme highlighting all the possible reaction pathways due to electron and proton transfers[35,36] (Scheme 1). Depending on the pH of the solution, the reaction can proceed along different pathways and the formation of specific inter-

(20) Alessandrini, A.; Gerunda, M.; Canters, G. W.; Verbeet, M. P.; Facci, P. *Chem. Phys. Lett.* **2003**, *376*, 625–630.
(21) Alessandrini, A.; Salerno, M.; Frabboni, S.; Facci, P. *Appl. Phys. Lett.* **2005**, *86*, 133902.
(22) Alessandrini, A.; Corni, S.; Facci, P. *Phys. Chem. Chem. Phys.* **2006**, *8*, 4383–4397.
(23) Chi, Q.; Farver, O.; Ulstrup, J. *Proc. Natl. Acad. Sci. U.S.A.* **2005**, *102*, 16203–16208.
(24) Davis, J. J.; Peters, B.; Xi, W. *J. Phys.: Condens. Matter* **2008**, *20*, 374123.
(25) Schmickler, W. *Surf. Sci.* **1993**, *295*, 43–56.
(26) Zhang, J.; Chi, Q.; Albrecht, T.; Kuznetsov, A. M.; Grubb, M.; Hansen, A. G.; Wackerbarth, H.; Welinder, A. C.; Ulstrup, J. *Electrochim. Acta* **2005**, *50*, 3143–3159.
(27) Kuznetsov, A. M.; Schmickler, W. *Chem. Phys.* **2002**, *282*, 371–377.
(28) Schmickler, W.; Tao, N. *Electrochim. Acta* **1997**, *42*, 2809–2815.
(29) Zhang, J.; Chi, Q.; Kuznetsov, A. M.; Hansen, A. G.; Wackerbath, H.; Christensen, H. E. M.; Andersen, J. E. T.; Ulstrup, J. *J. Phys. Chem. B* **2002**, *106*, 1131–1152.
(30) Friis, E. P.; Kharkats, Y. I.; Kuznetsov, A. M.; Ulstrup, J. *J. Phys. Chem. A* **1998**, *102*, 7851–7859.
(31) Kuznetsov, A. M.; Medvedev, I. G. *Electrochem. Commun.* **2008**, *10*, 1191.
(32) Kuznetsov, A. M.; Medvedev, I. G.; Ulstrup, J. *J. Chem. Phys.* **2009**, *131*, 164703.
(33) Albrecht, T.; Guckian, A.; Kuznetsov, A. M.; Vos, J. G.; Ulstrup, J. *J. Am. Chem. Soc.* **2006**, *128*, 17132–17138.
(34) Chamber, J. Q. In *The Chemistry of the Quinonoid Compounds*; Patai, S., Ed.; Wiley: New York, 1974; pp 737−792.
(35) Jacq, J. *Electrochim. Acta* **1967**, *12*, 1345–1371.
(36) Laviron, E. *J. Electroanal. Chem.* **1984**, *164*, 213–227.

Scheme 1. Nine-Membered Scheme for the Overall Reaction from Benzoquinone to Hydroquinone[a]

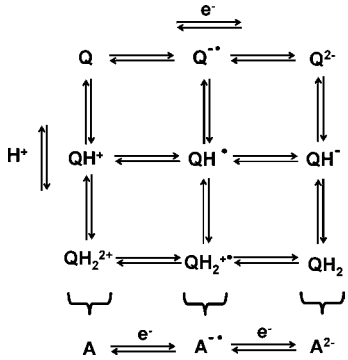

[a] Each transition is characterized by its redox equilibrium potential and p*K*. Under protonation equilibrium, the overall reaction is kinetically equivalent to two reactions characterized by the transfer of one electron and by an apparent redox potential.

mediates can be the rate-limiting step of the reaction. In our experiments, we used a buffered solution to perform all the measurements and it is well-known that under such conditions the electrochemical reaction proceeds via the $2e^-$ and $2H^+$ transfer mechanism.[37] Because of the involvement of protons in the redox reaction, the equilibrium distribution between the two species is pH dependent, shifting to more negative potentials as the pH increases. This behavior suggests that the hydroquinone molecule could be used as a molecular switch triggered by a pH change. To the best of our knowledge, this is the first time that a redox couple involving the exchange of two electrons and protons is studied by EC-STM. In this report, we show tunneling enhancement in the interfacial electron transfer process between the tip and the substrate via the hydroquinone-derivatized molecules. In particular, two regions of enhancement, symmetrically positioned with respect to the equilibrium redox potential of the hydroquinone/quinone couple, are found. We also demonstrate how this electron transfer mechanism can be interpreted according to the current EC-STM theoretical framework. We show that the two observed regions of tunneling enhancement are due to two electron transfer processes involving one electron and occurring at potential values strictly related to pH.

2. Experimental Section

2.1. Sample Preparation. 2-(6-Mercaptoalkyl)-hydroquinone (H_2Q-$(CH_2)_6$-SH) was synthesized according to the procedure reported in ref 38. Au(111) substrates were prepared by evaporating a 150 nm-thick gold layer on mica substrate preanneled at 450 °C in high vacuum and subsequently annealed at the same temperature for 4 h in high vacuum. For assembling the hydroquinone self-assembled monolayer (SAM), a gold substrate was flame annealed and immediately immersed in an ethanol solution containing the molecules to form the SAM. For EC-STM imaging a SAM was assembled on Au(111) starting from an ethanol solution composed of 10 μM 6-mercapto-1-hexanol (MCH) and 10 μM H_2Q-$(CH_2)_6$-SH with an overnight incubation. After the incubation, the sample was copiously rinsed in ethanol and mounted in the EC-STM cell. The imaging buffer was 50 mM NH_4Ac, pH 4.6. This preparation yielded a monolayer characterized by the presence of bumps protruding from a background in the EC-STM images. These bumps can be interpreted as single molecules or small islands of derivatized hydroquinone molecules protruding above the MCH layer (Scheme 2). For Electrochemical Scanning Tunneling Spectroscopy (EC-STS), the sample was assembled by incubating a freshly annealed Au(111) substrate in a 10 μM $H_2Q(CH_2)_6$-SH ethanol solution overnight (Scheme 2). Then, the sample was abundantly rinsed in ethanol and installed in the EC-STM cell. The buffers used for EC-STS were 50 mM NH_4Ac, pH 4.6, and 50 mM NH_4Ac, pH 7.6.

2.2. Electrochemical Characterization, EC-STM Imaging, and Scanning Tunneling Spectroscopy (STS). The derivatized hydroquinone SAMs were characterized by cyclic voltammetry. Electrochemical data were acquired under the same conditions as for EC-STM and STS in order to facilitate comparison. The buffers used for cyclic voltammetry were all 50 mM NH_4Ac at four different pH values: 4.6, 5.6, 6.6, and 7.6.

EC-STM imaging was performed with a PicoSPM microscope (Molecular Imaging) equipped with a bipotentiostat. The bipotentiostat allowed to control independently the potential of both substrate and tip with respect to a quasi-reference silver wire in the imaging cell. The tip was obtained by first chemically etching a Pt/Ir (80/20) wire followed by coating with Apiezon wax to minimize leakage currents to values smaller than 5−10 pA. A Pt wire was used as counter electrode. At the beginning and at the end of each experimental session, the reference potential of the silver wire was checked against a SCE reference electrode and all the data in the following sections are referred to SCE. For spectroscopy-like imaging, a sequence of images of the same sample area was acquired at constant bias for different values of the substrate potential. The sample was a SAM obtained from a mixture of mercaptohexanol (MCH) and ($H_2Q(CH_2)_6$-SH) on Au(111) (see Sample Preparation section). The apparent height variation of the hydroquinone-terminated molecules observed upon varying the substrate potential was measured against the electrochemically inactive MCH molecules. For EC-STS, the variation of I_t upon substrate potential (V_s) was measured at fixed height and lateral tip position on a sample composed of a SAM of $H_2Q(CH_2)_6$-SH on Au(111). The tip−substrate approach was performed as usual at a given tunneling current set point and the feedback loop was then switched off. The starting substrate potential was based on the spectroscopy-like imaging data and chosen to avoid enhancement in tunnelling current (0 V). The substrate potential was then swept alternately toward the positive and negative direction in order to cross the redox potential of the hydroquinone/benzoquinone couple. Comparison of the tunneling current at the beginning and at the end of the sweep was used as a marker of vertical stability of the tip/substrate position. STS experiments were also performed at different bias voltages.

3. Results and Discussion

3.1. Electrochemistry of the Hydroquinone-Containing Monolayers. Previous investigation of SAM on gold of alkylthiol derivatives of the hydroquinone/quinone couple involved electrochemical characterizations[38−40] and FT Infrared Spectroscopy[41] to study the reorganization of the molecular structure as a function of the oxidation state. To study the electrochemical properties of the molecules used in our work, we formed monolayers of $H_2Q(CH_2)_6$-SH on Au(111) substrates. Cyclic voltammetry characterization was performed in the same buffer used for EC-STM investigations. It is well established that in buffered solutions the redox reaction proceeds via a $2e^-$, $2H^+$ transfer mechanism. Figure 1 shows typical voltammograms obtained at different scan rates for the hydroquinone-containing

(37) Quan, M.; Sanchez, D.; Wasylkiw, M. F.; Smith, D. K. *J. Am. Chem. Soc.* **2007**, *129*, 12847–12856.
(38) Park, W.; Hong, H. G. *Langmuir* **2001**, *17*, 2485–2492.
(39) Larsen, A. G.; Gothelf, K. V. *Langmuir* **2005**, *21*, 1015–1021.
(40) Park, W.; Hong, H. G. *Bull. Korean Chem. Soc.* **2006**, *27*, 381–385.
(41) Sato, Y.; Fujita, M.; Mizutani, F.; Uosaki, K. *J. Electroanal. Chem.* **1996**, *409*, 145.

Scheme 2[a]

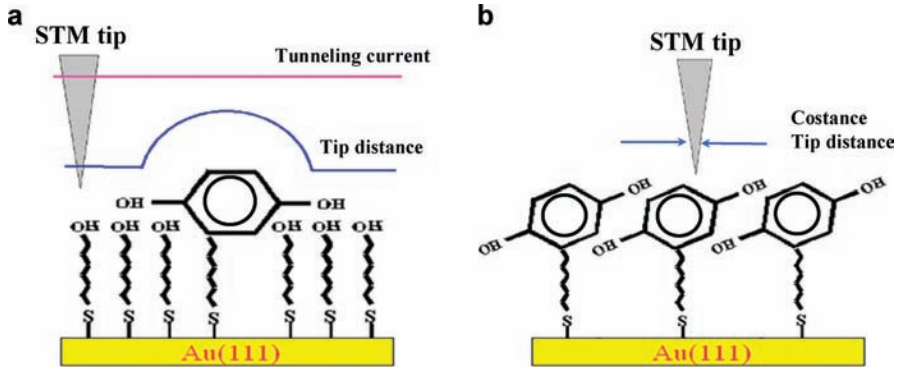

[a] (a) Mixed Self Assembled Monolayer of MCH and $H_2Q(CH_2)_6$-SH on Au(111) used to perform spectroscopy-like EC-STM. The orientation of the chains does not necessarily coincide with the real one. (b) Monolayer of $H_2Q(CH_2)_6$-SH on Au(111) used to perform STS experiments.

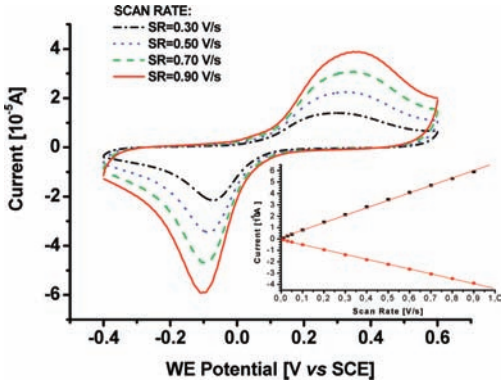

Figure 1. Voltammograms of a mixed MCH/$H_2Q(CH_2)_6$-SH monolayer in 50 mM NH_4Ac pH 4.6 for different scan rate values (from 0.3 to 0.9 V/s). The inset shows the linear dependence of the current on the potential scan rate to highlight the presence of a surface confined redox species.

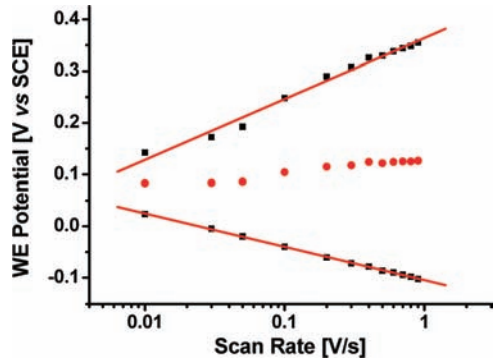

Figure 2. Position of the cathodic and anodic peaks of the voltammograms as a function of the potential scan rate. Also the redox midpoint is reported as a function of the scan rate.

monolayer in 50 mM NH_4Ac at pH 4.6. The redox peak current scales linearly with the voltage scan rate (inset to Figure 1) as expected for a surface bound redox species. The anodic and cathodic peaks observed at a scan rate of 100 mV/s are separated by 300 mV in accordance with ref 38 for the same molecule in 0.1 M $HClO_4$ solution. This separation highlights the irreversibility of the electron transfer process due to the length of the spacer and the related slow electron transfer rate. The formal potential E_0 is (0.10 ± 0.01) V. In Figure 2, we investigated the dependence of the peak positions as a function of the voltage scan rate. An asymmetry is present in the behavior of the anodic and cathodic peaks as a function of the scan rate. We used the Laviron's formalism to analyze the results for the regions with a peak separation higher than 200 mV.[42] The analysis allowed us to calculate the number of electrons transferred in the redox reaction of the hydroquinone/quinone couple, obtaining a figure of 1.6. This value is slightly less than the expected value of 2 but still in accordance with what was reported in other studies on the same system in more acidic solutions.[40,43] The lower average number of electrons exchanged with respect to the theoretical value could be related to a nonsymmetric energy barrier for the redox reactions involving the hydroquinone/quinone couple. Indeed, the Laviron formalism exploited to obtain the transfer rate constant and the number of exchanged electrons usually assumes the same electron transfer coefficient for the anodic and cathodic peaks.

A previous work on $H_2Q(CH_2)_n$-SH SAMs on gold allowed to estimate the reorganization energy λ of the electrochemical redox reaction for the hydroquinone/quinone couple.[40] By studying the electrochemical reaction as a function of temperature, a figure of 1.3−1.4 eV was obtained for this redox couple. The large value obtained can be explained on the basis of the molecular structural changes occurring during the redox reaction. For the hydroquinone/quinone reaction, a large internal structural reorganization of the molecule is required, and a large contribution to the overall reorganization energy is expected from the inner-sphere part. This is in contrast to redox reactions where the molecular geometric changes upon redox state variations are negligible. It must be pointed out that in the EC-STM configuration the presence of the STM probe can influence the outer-sphere contribution to the reorganization energy leading to its reduction as the tip is moved closer to the substrate.[44] In our EC-STM investigation, the redox-active molecules display a high value of the inner-sphere reorganization energy and this must be taken into account in the theoretical analysis of the results.

The proton-coupled electron transfer reaction for the hydroquinone/quinone redox couple has electrochemical characteristics dependent on the pH of the solution. This behavior bears an interesting effect on our system, since pH changes could be used to gate the electronic conductance of the molecules. Figure 3a shows the voltammograms of the $H_2Q(CH_2)_6$-SH monolayer on gold obtained at four different pH values of the 50 mM

(42) Bortolotti, C. A.; Battistuzzi, G.; Borsari, M.; Facci, P.; Ranieri, A.; Sola, M. *J. Am. Chem. Soc.* **2006**, *128*, 5444–51.
(43) Park, W.; Ahmed, J.; Kim, S. *Colloids Surf., B* **2009**, *68*, 120–4.
(44) Corni, S. *J. Phys. Chem. B.* **2005**, *109*, 3423–30.

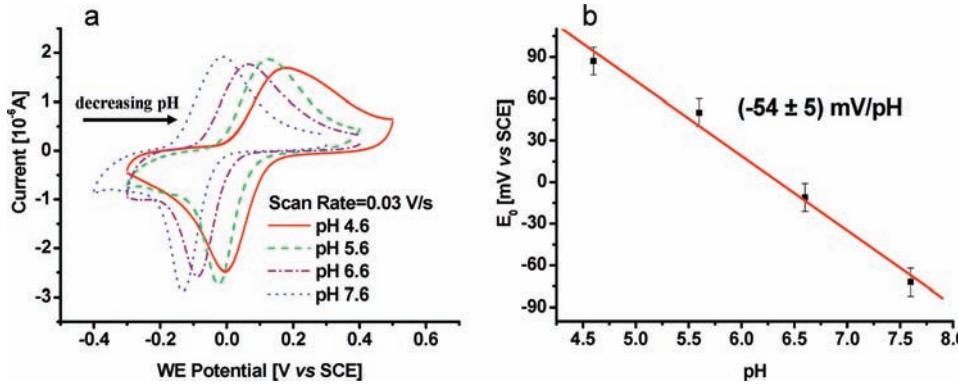

Figure 3. (a) Cyclic voltammograms of SAM of $H_2Q(CH_2)_6$-SH obtained at a scan rate of 0.03 V/s in 50 mM NH_4Ac for four different pH values: 4.6, 5.6, 6.6, and 7.6; (b) dependence of E_0 position as a function of pH. The obtained linear shows a slope equal to (-54 ± 5) mV/pH.

NH_4Ac solution. In Figure 3b, the position of the anodic and cathodic peaks obtained, along with the E_0, are reported as a function of pH at the same scan rate (0.03 V/s). From the plots, it can be inferred that an increase of the pH results in a decrease of the peak separation. The plot of E_0 as a function of pH shows a slope equal to -54 ± 5 mV/pH, whereas the theoretical value for a two electrons/two protons reactions is -59 mV/pH. This small difference could be interpreted as the result of the different pK_a for the hydroquinone/quinone SAM with respect to the corresponding pK_a value in solution.[45] At low pH, the monolayer will mainly display QH_2 moieties and the oxidation will involve the exchange of two protons and two electrons. As the pH increases, the monolayer will be partially in the deprotonated state and the reaction will correspondingly involve a decreasing number of protons (one or none) and two electrons. It is, however, worth pointing out that, if the number of involved protons changes with pH, a variation in the slope of the E_0 versus pH around the expected pK_a for the surface species should be observed. In our experiments, we did not observe any changes in the E_0 versus pH slope in the plot. We interpreted this observation as an indication that the pK_a of the SAM was not reached and that the electron transfer for this system consists of the exchange of two electrons and two protons.

For EC-STM imaging, the hydroquinone monolayer was assembled in mixed form with OH terminated alkylthiols containing the same number of CH_2 groups in the alkylic chain. To correctly interpret the EC-STM images with respect to STS experiments, we investigated the electrochemical characteristics of the mixed bilayer. The mixed SAM results in the dilution of the electroactive molecules which, as a consequence, do not influence each other during the redox reaction. The electrochemical characteristics of the mixed monolayer are not substantially different from those of the $H_2Q(CH_2)_6$-SH monolayer. Decrease in both peak width and background current was observed for the mixed SAM, while E_0 was not significantly different from that observed for the homogeneous SAM.[39]

3.2. EC-STM Imaging. EC-STM imaging was performed in constant-current mode on the mixed SAM assembled with MCH and $H_2Q(CH_2)_6$-SH. In the spectroscopy-like imaging, a sequence of images of the same sample area was obtained at constant bias while varying the substrate potential. In this experiment, a variation in the conductance of the imaged redox molecules upon varying the substrate potential would be reflected in a difference in apparent height with respect to the background. In Figure 4a−d, a sequence of images for the substrate potential between -0.37 and 0.34 V for a V_{bias} of 400 mV is reported at the same *z*-scale for each image. Small lighter spots emerged from the background and were interpreted as single molecules or small islands of derivatized-hydroquinone molecules. It must be noted that the spots' apparent height with respect to the MCH background was dependent on the substrate potential. In Figure 4e, we reported the line sections across the same molecular feature (highlighted in the images of Figure 4a−d) for the different values of the substrate potential. Averaging the apparent height over 10 spots yielded the trend reported in Figure 4f. For a substrate potential of -0.3 V versus SCE, a maximum in the apparent height was obtained indicating resonant-like behavior resulting from increased conductivity of the molecules.[46] For a substrate potential around the redox midpoint of the hydroquinone/quinone couple, a relatively constant height was observed. Going toward positive potentials, a small increase in conductivity was noted and could be interpreted as the beginning of a new maximum. With this approach, the real tunnelling enhancement cannot be measured because imaging is performed at constant tunnelling current and the current variation can be established only if the tunnelling decay length at each tip location is known. The observed bumps cannot be easily attributed to single molecules or islands composed of a small number of molecules. In particular, the number of molecules involved in the electron transfer mechanism could be relevant for a more quantitative interpretation of the interfacial electron transfer mechanism in terms of single molecule conductance and number of electrons exchanged per second. In this work, we are mainly interested in the value of substrate potential at which the maximum in the tunnelling enhancement occurs. A statistical analysis on the tunnelling current peak intensities in EC-STS would be required to establish the number of molecules involved in the tunneling area, but this estimation is beyond the scope of this work.

3.3. Electrochemical Scanning Tunneling Spectroscopy (EC-STS). Direct access to the tunnelling current can be obtained by performing a scanning tunnelling spectroscopy study in electrochemical environment. To this aim, an Apiezon insulated tip was brought in within tunnelling distance under feedback control until a target set point current was obtained. The substrate potential of 0 V used during tip substrate approach

(45) Brooksby, P. A.; Schiel, D. R.; Abell, A. D. *Langmuir* **2008**, *24*, 9074–9081.

(46) Tsoi, S.; Griva, I.; Trammell, S. A.; Blum, A. S.; Schnur, J. M.; Lebedev, N. *ACS Nano* **2008**, *2*, 1289–1295.

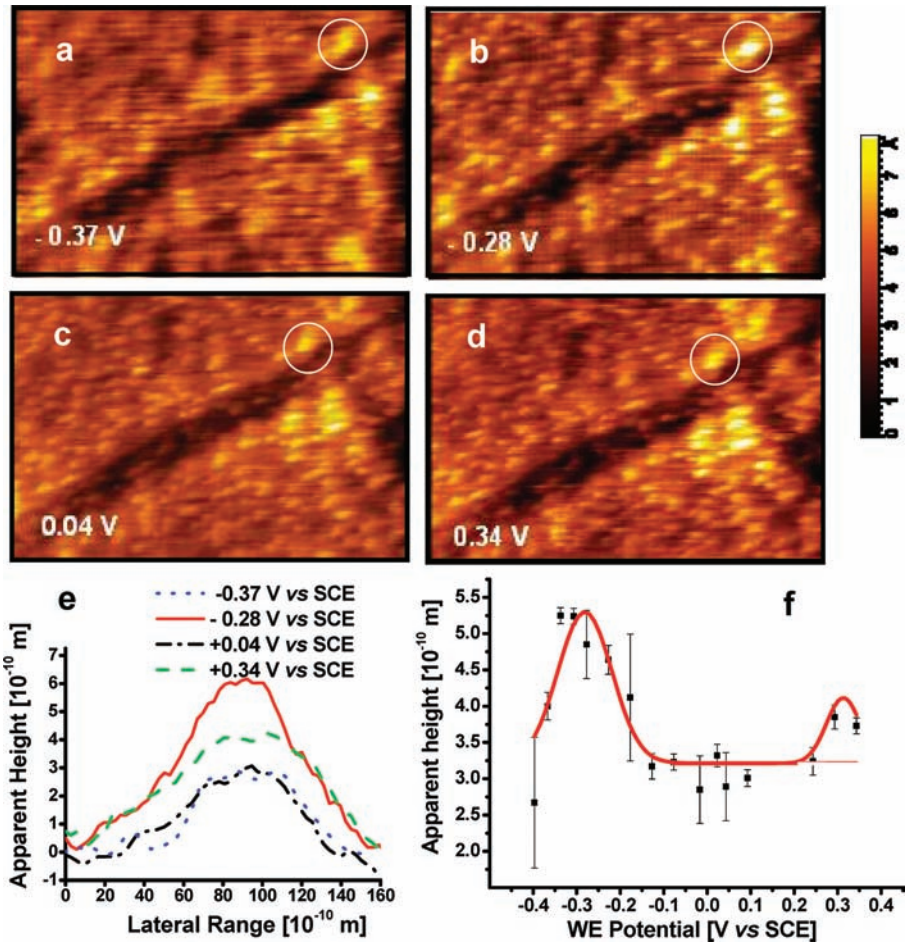

Figure 4. (a−d) Sequence of four EC-STM images obtained with a V_{bias} of 400 mV and $I_{setpoint}$ = 1 nA for different substrate potential. The substrate potential vs SCE is reported in each image. The images were acquired in 50 mM NH_4Ac pH 4.6. Image size: 120 × 80 nm^2. (e) Cross sections of the same molecular feature (highlighted by white circles in the images) for different values of the substrate potential. (f) Apparent height of the quinone molecules with respect to the nonelectrochemical MCH adlayer as a function of the substrate potential. The solid line has been introduced as a guide to the eye to highlight the tunneling enhancement regions. Error bars correspond to two standard deviations obtained from the measurement of 10 spots in the images at each substrate potential.

was chosen based on the spectroscopy-like imaging results and positioned as it lays in a region of no tunnelling enhancement. Subsequently, the feedback control was disabled and curves for I_t versus V_s at constant bias were acquired in the range -0.4 V $< V_s < 0.6$ V. Under these conditions, the Fermi energy levels of the two working electrodes (the tip and the substrate) are shifted relative to the redox levels of the molecules at the surface. Figure 5 shows a curve obtained for an engage set point of 0.5 nA and a V_{bias} of 100 mV. The curve has been overlaid to the observed behavior for the apparent height at a V_{bias} of 400 mV and a current set point of 1 nA. The I_t versus V_s curve clearly shows the presence of two peaks. The peak obtained for negative potentials is located at almost the same substrate potential than that for the apparent height behavior. The peak observed for positive potentials in the tunnelling spectroscopy experiment is located at the same potentials where an additional increase in the apparent height seemed to rise. The correspondence of the peak positions in both experiments is convincing evidence that the same electron transfer mechanism is at play. It is important to note hat the positions of the peaks were largely independent of both the scan direction and the scan rate in the range we could test (0.03−0.05 V/s). The STS trace baseline shows an increasing conductance of the molecules as the potential is moved to negative values. This behavior can be rationalized on the basis of an increased conductance of quinone in its reduced form. A similar behavior has been obtained for viologen based molecules.[18]

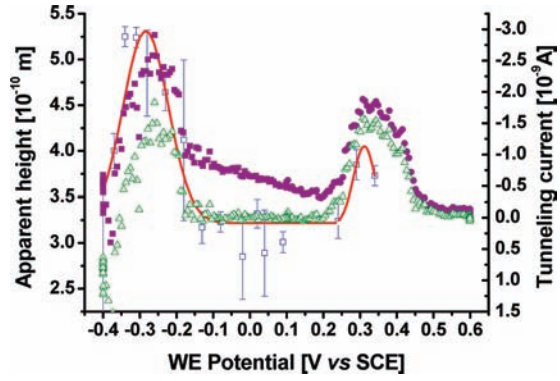

Figure 5. EC-STS curves obtained for V_{bias} = 100 mV, approaching set point current of 0.5 nA and scan rate 0.03 V/s. The filled points show the raw data. The empty triangles points are obtained from the filled ones after removal of the baseline. The empty squares represent the behavior of the apparent height data obtained from spectroscopy-like imaging with the continuous line introduced as a guide to the eye.

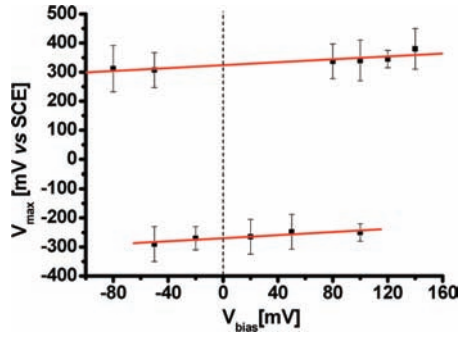

Figure 6. Position of the maxima of the tunneling current as a function of applied bias for the positive peak (upper data) and the negative one (lower data).

We then studied the behavior of the tunneling current enhancement for different values of the applied V_{bias} for both peaks. Figure 6 shows the dependence of the location of the I_t maximum, obtained after fitting a Gaussian curve to the data with respect to the V_{bias} in the case of the positive and negative peaks. A linear dependence was found with an intercept for $V_{bias} = 0$ V corresponding to a potential of (324 ± 60) mV for the positive peak and (-270 ± 30) mV for the negative one.

Previous studies by EC-STM together with theoretical models of the interfacial electron transfer mechanism established that the electron transfer mechanism involved is likely the two step model with partial vibrational relaxation of the redox molecule between the first and the second step. In this case, an expression for the tunnelling current is the following (eq 1):[47]

$$I = e\kappa\rho(eE_{bias})\frac{\omega}{2\pi} \times \left\{ \exp\left[\frac{e}{4\lambda kT}(\lambda/e + \xi\eta + \gamma E_{bias})^2\right] + \exp\left[\frac{e}{4\lambda kT}(\lambda/e + E_{bias} - \xi\eta - \gamma E_{bias})^2\right] \right\}^{-1} \quad (1)$$

where e is the electron charge, κ is the electronic transmission coefficient, ρ is the density of electronic states in the metal electrodes, ω is the nuclear vibration frequency, λ is the reorganization energy, $\eta = E_s - E_0$ is the difference between the substrate potential and the equilibrium redox potential of the redox species (overvoltage), k is the Boltzmann constant, T is the temperature and ξ and γ are two parameters ranging between 0 and 1 which describe the effective electrode potential as a function of η and E_{bias}, respectively. Under the conditions of low E_{bias} and η, we obtain an expression for the voltage position of the tunnelling maximum given by (eq 2):[18]

$$E_{max} = E^0 + \left(\frac{1}{2} - \gamma\right)\frac{E_{bias}}{\xi} \quad (2)$$

Equation 2 can be exploited to analyze the data illustrated in Figure 6. Performing a fit of eq 1 to the data obtained for the tunneling current enhancement experiment, we can obtain a best estimate for parameters ξ, γ, and λ. Unfortunately, these parameters are strictly interconnected and they cannot be determined independently. The same consideration holds true for eq 2. Considering the positive slope of the tunneling maxima positions versus the applied bias voltage, it can be argued that γ should range between 0 and 0.5. For values of γ lower than 0.5, the fit to the tunneling current described by eq 1 is not very responsive to the specific value for γ. In these cases, the estimated values for ξ and λ are 0.6 and 0.3 eV, respectively, and are both physically meaningful. However, the values obtained for ξ and γ do not reproduce the parameters of the linear behavior of eq 2. This could result from the approximations introduced to obtain eq 2, which are not completely satisfied in our case (E_{bias}, $\eta \ll \lambda$). The estimated value for λ is, however, significantly lower than that obtained by electrochemical studies[40] of 1.4 eV. The lower value obtained for the reorganization energy λ with the EC-STM setup can be ascribed to a reduced solvent accessibility due to the proximity of the STM tip as this can reduce the contribution of the solvent reorganization to the overall reorganization energy. However, the lower value could also be the result of an electron transfer mechanism involving only the half reaction of the benzoquinone to hydroquinone redox couple.

The presence of two tunneling current enhancement regions raises the question of whether they are both due to the same redox species or if they are due to two different species with different equilibrium potentials. According to theories developed to understand the interfacial electron transfer mechanism, two peaks could be expected due to electron and hole transfer, respectively (see Introduction). If both peaks are due to the same species, it can be assumed that this would be the hydroquinone/benzoquinone redox couple, even if its redox equilibrium potential is far from the peak positions. Otherwise, if the two peaks are due to two different species, we are limited by the fact that we cannot have direct access to the redox equilibrium positions of the two species from the electrochemical characterization. Considering the two-step electron transfer process for a one electron interfacial exchange reaction, we can obtain the redox midpoint of both species by extrapolating to $V_{bias} = 0$ the linear trend of the peak position versus V_{bias} (Figure 6).

To shed light into the presence of one or two electroactive species trying to better understand the charge transfer mechanism, we studied the effect of pH on the observed features.

3.4. Effect of pH. Having established that the electrochemical behavior of the quinone modified electrode depends on the pH of the solution and considering the relationship between tunneling enhancement behavior and electrochemical characteristics of redox molecules, it is to be expected that, if the two peaks obtained in this experiment are due to different chemical species, their behavior as a function of pH should also be different. As a result the redox potential for each species should show a different pH-dependence. To test this assumption, we performed EC-STS measurements in NH_4Ac at pH 7.6. The results, compared to those at pH 4.6, are reported in Figure 7. It is evident that at pH 7.6 the positive peaks shift toward negative potential by a quantity roughly corresponding to the expected potential variation of the redox species (−54 mV/pH). On the other hand, the negative peak does not shift and this behavior suggests that the two peaks stem from two different species.

The electrochemistry of the hydroquinone/benzoquinone redox couple has been extensively studied by Laviron in the 1980s. The peculiarity of proton transfer coupled to electron transfer leads to specific kinetic pathways dictated by the availability of protons in the solution. In buffered solution, the electrochemical reaction proceeds with a transfer of $2e^-$ and 2 H^+. The nine-membered Scheme 1 is characterized by a standard redox potential and pK_a for each of the nine species. When

(47) Kuznetsov, A. M.; Ulstrup, J. *J. Electroanal. Chem.* **2004**, *564*, 209–222.

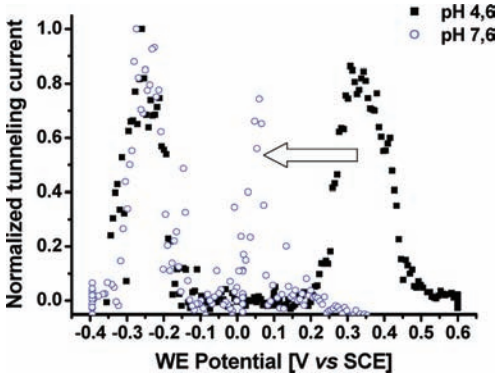

Figure 7. EC-STS measurements performed in NH_4Ac at pH 4.6 (filled squares) and pH 7.6 (empty circles). The curves have been obtained at V_{bias} = 100 mV and $I_{setpoint}$ = 0.5 nA.

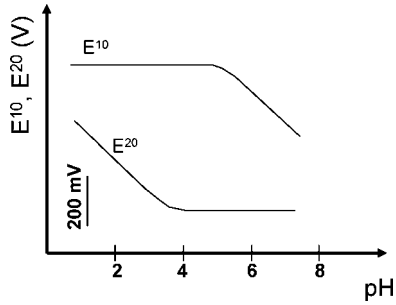

Figure 8. Schematics of the variation of the two apparent redox potentials upon pH variation as deduced from the kinetic analysis by Laviron (modified from ref 36, Figure 5).

protonation reactions are at equilibrium, the nine-member reaction behaves kinetically as two single reactions each involving a one-electron exchange characterized by a corresponding apparent redox potential (E^{10}, E^{20}). The model by Laviron predicts a different behavior for the two redox potentials as a function of pH which is schematically illustrated in Figure 8. This theoretical model agrees with the analysis of the data obtained by Vetter.[48] The separation between the two apparent equilibrium redox potentials at pH 4.6 is about 600 mV as deduced from Figure 8 and this is consistent with the distance in mV that we observed between the two peaks by EC-STM at the same pH. The predictions by Laviron show that by increasing the pH to 7.6 the peak at higher potential moves to lower potentials, while the lower potential peak remains at a constant value. This is exactly what we observed in our EC-STS investigation at different pH values. The different behavior observed for the two tunneling current enhancements upon pH variation strongly supports the idea that they result from the equilibrium redox potential of two different species and that they are connected by the two one-electron reactions foreseen by the Laviron model. According to this interpretation, the tip/molecule/substrate interfacial electron transfer mechanism allows the visualization of intermediate states of the nine-membered reaction scheme that are not evident in the voltammetric wave. In fact, the cyclic voltammograms showed only one oxidation/reduction wave corresponding to a number of exchanged electrons close to 2, indicating that the reaction intermediates are not stable. This observation is typical of mechanisms where the second electron transfer step is much faster than the first one.[49]

From a theoretical standpoint, the proton-independent two-electrons tunneling mediated by one redox level has been studied recently by Kuznetsov et al.[31,32] This treatment is also relevant for cases involving multielectron systems.[50] In this case, the model relates to the Coulomb blockade effect resulting from the interaction between the two electrons located in the redox group. The appearance of two regions of tunneling enhancement has been predicted for the tunneling current versus overpotential relation. This represents the presence of three oxidation states of the molecule rather than two. The molecule can in fact accept zero, one, or two electrons. The occurrence of two maxima has also been associated to the presence of two levels in the bridging molecule.[51] In the latter case, the levels are sequentially available and the redox groups display the same levels. When the electronic coupling between the redox groups is higher than the interaction of the groups with the electrodes, two maxima are observed. The two peaks are positioned almost symmetrically with respect to the equilibrium redox potential resulting from the strong interaction between the two groups and this gives rise to a splitting of the redox levels equivalent to the formation of bonding and antibonding levels. It has also to be noted that in a redox reaction the reorganization of the reaction medium contributes to lower significantly the effect of the Coulomb repulsion when two electrons are involved. The tip effect in the EC-STM setup usually reduces the reorganization energy connected to the medium due to partial volume exclusion by the tip. As a consequence, the effective Coulomb repulsion for the two electrons in the molecule increases. In this situation, it is possible that the transfer of the two electrons occurs via intermediate states each involving the transfer of only one electron. Moreover, the rate transfer of the hydroquinone/benzoquinone redox couple in the SAM is quite slow ($k_{s,app} \sim 5 \times 10^{-1}$ s^{-1}), whereas the tunneling current in the EC-STS measurements implies that about 10^9 electrons are injected through the redox molecule resulting in a higher transfer rate with respect to Cyclic Voltammetry. According to this consideration, Coulomb blockade effects could play a role in the observed behavior.

4. Conclusions

In this work, we demonstrated that the tunneling resistance of the STM tip/hydroquinone/substrate junction can be modulated by exploiting the concept of electrolyte gating for redox molecules. The exchange of two electrons and two protons characteristic of the hydroquinone/benzoquinone redox couple leads to the appearance of distinguishing features in the tunneling current/overpotential relation in the EC-STM configuration. While in bulk electrochemical analysis it is not possible to observe a reaction where the two electrons are seen as separate transitions, with the *in situ* STM configuration, both the EC-STM spectroscopy-like imaging and the EC-STS experiments show the presence of two regions of tunneling enhancement that can be attributed to the separate transfer of the two electrons. This could be ascribed to the possibility of EC-STM

(48) Vetter, K. J. *Z. Electrokem.* **1952**, *56*, 797.
(49) Bard, A. J.; Faulkner, L. R. *Electrochemical Methods: Fundamentals and Applications*; Wiley: New York, 2001.
(50) Albrecht, T.; Mertens, S. T. L.; Ulstrup, J. *J. Am. Chem. Soc.* **2007**, *129*, 9162–9167.
(51) Kuznetsov, A. M.; Medvedev, I. G. *J. Phys.: Condens. Matter* **2008**, *20*, 374112.

to detect the presence of every redox level pertaining the molecule situated between the tip and the substrate. When injecting electrons through the molecule, the presence of the redox levels produces tunneling current enhancements. Moreover, as the reaction involves also the exchange of protons, the regions of tunneling enhancement for the substrate potential can be shifted by modifying the pH of the solution. Thus, pH can be considered as an additional parameter to gate the tunneling current in the studied junction.

Acknowledgment. The authors thank Dr. Stefano Corni for very useful discussion about the work. Italian MIUR Project FIRB2007 "Italnanonet" n. RBPR05JH2P, is gratefully acknowledged.

JA101666Q